Detecting Driver Sleepiness from EEG Alpha Wave during Daytime Driving

Yingying Jiao
Department of Computer Science and Engineering
Shanghai Jiao Tong University
Shanghai, China
jiaoyingying2010@163.com

Bao-Liang Lu*
Department of Computer Science and Engineering
Shanghai Jiao Tong University
Shanghai, China
bllu@sjtu.edu.cn

***Abstract*—Drowsy driving is the main reason for sleep-related crashes. We have observed that an alpha wave attenuation-disappearance phenomenon and a typical alpha blocking phenomenon commonly exist in the eye closure events during daytime simulated driving experiments. These two alpha-related phenomena prove to respectively represent two different sleepiness levels: the sleep onset and the relaxed wakefulness. Therefore, we propose a novel algorithm for tracking the alpha wave change and detecting the two alpha-related phenomena in real-time for recognizing driver sleepiness. Our proposed algorithm adopts continuous wavelet transform for charactering the signal change and support vector machine for classification. The experimental results indicate that the algorithm is able to detect the start and end points of alpha waves during eye-closed period and distinguish the two types of end points of alpha waves in two alpha-related phenomena with high sensitivity and precision. The eye-closed period detected by our algorithm with alpha waves has a high overlapping rate with that marked by human experts. The main contributions of the proposed algorithm are twofold: to detect alpha waves during the eye-closed period in real-time and serve as an indicator for judging the current sleepiness level as the sleep onset or relaxed wakefulness at the end points of alpha waves.**

***Index Terms*—Sleep onset period, alpha blocking, alpha attenuation, continuous wavelet transform, driver sleepiness**

I. Introduction

Falling asleep at the wheel accounts for numerous road crashes under the monotonous driving condition and thus finding a reliable physiological indicator for recognizing the driver's sleepiness is meaningful. The attenuation of EEG alpha waves is reported to be the most valid electro-physiological marker of sleep onset period (SOP) by numerous sleep-related studies [1], [2]. The Hori's nine-stage system is validated to be particularly useful for precisely describing SOP. In Hori's sleep stage H1, the EEG data epoch is dominated by a train of alpha activity but in Hori's sleep stage H2 and H3 alpha waves present intermittent form with the percentage of alpha activity decreasing from more than 50% to less than 50% [1]. However, during driving, the eyes keep open in most of the time and the change characteristics of alpha waves have not been studied fully until now. Our previous work [3] has found an new alpha attenuation-disappearance phenomenon and proven that this phenomenon exists as a general pattern for predicting the entry into sleep during daytime simulated driving. This alpha attenuation-disappearance phenomenon as well as the typical alpha wave blocking phenomenon [4], which is well known to appear during relaxed wakefulness [4], [5], were both observed during our simulated driving. Obviously, the alpha wave attenuation-disappearance and alpha blocking phenomena respectively represent two significantly different sleepiness levels: the sleep onset and the relaxed wakefulness. Therefore, we propose a novel algorithm, which combines the continuous wavelet transform and the support vector machine (SVM) classifier, to track alpha wave's change and distinguish these two types of alpha-related phenomena.

*Corresponding author: Bao-Liang Lu. This work was supported by the National Key Research and Development Program of China (2017YFB1002501), the National Natural Science Foundation of China (61272248), the Major Basic Research Program of Shanghai Science and Technology Committee (15JC1400103), the ZBYY-MOE Joint Funding (6141A02022604), and the Technology Research and Development Program of China Railway Corporation (2016Z003-B).

II. Materials

A. Experiment Procedure

Eight subjects (5 males and 3 females, aged 23 $\pm$ 1.5) who had the siesta habit were recruited. The Epworth Sleepiness Scale [6] was used to measure the subjects' general level of daytime sleepiness. The mean $\pm$ SD of ESS scores for eight subjects is 10.5 $\pm$ 1.2. Each experiment started half an hour before the regular sleep time of the subjects at noon and lasted for about two hours. The experimental task was just to keep the normal driving process like in real world, but closing eyes deliberately without feeling drowsy was strictly prohibited.

B. Data Recording

EOG and EEG signals were recorded at a 1000 Hz sampling rate using the ESI NeuroScan System. Totally, five electrodes were used, including two electrodes (Vu and Vd, which were receptively located above and below the left eye) for obtaining VEOG (VEOG = Vu-Vd) signal, one occipital electrode O2, one reference and one ground electrodes placed behind the ears. A camera was set to monitor the subject's face. In order to observe the eye movements and the corresponding EOG and EEG signals at the same time, the facial video from the camera and the EOG and EEG signals displaying on the Scan software interface, were synchronously recorded into a

978-1-5090-3050-7/17/$31.00 ©2017 IEEE

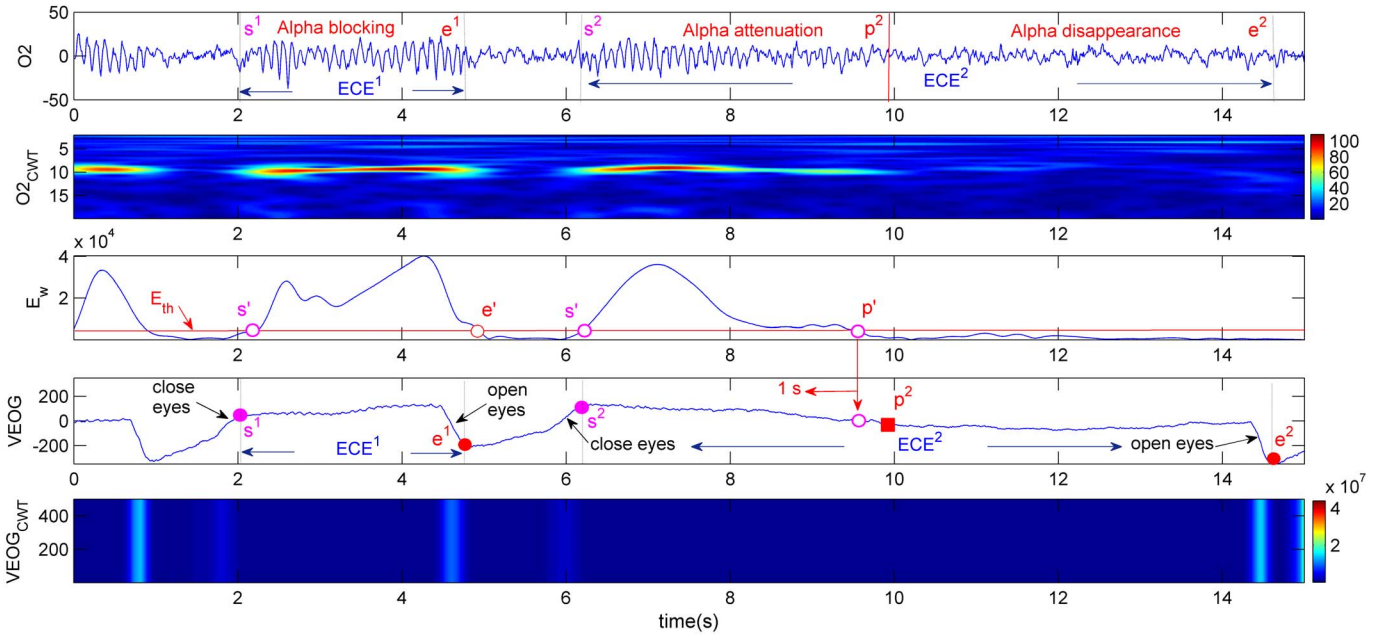

Fig. 1. Two types of alpha-related phenomena and the real-time detection process for the alpha wave change. Two types of eye closure events: ECE^1 and ECE^2. CWTs with complex Morlet wavelet and Haar mother wavelet are respectively used to obtain the time-frequency plots of the O2 and VEOG signals. E_w is the real-time change curve of alpha wavelet energy value.

file for reviewing and checking the relevance among the eye movements and the EOG and EEG signals.

III. Methods

A. Visual Marking for Two Alpha-related Phenomena

An eye closure event (ECE) was defined as the period between the end of upward trend line caused by closing eyes and the end of downward trend line caused by reopening eyes in VEOG signal, as shown in Fig. 1. There are only two types of eye closure events alternatively appearing in the simulated driving process: ECE^1 and ECE ^{2}. ECE^1 is defined as the eye closure event corresponding to alpha blocking phenomenon, usually appearing in the early stage of the simulated driving and still appearing in the later stage. The alpha blocking phenomenon refers to that alpha rhythm (8-12 Hz) activity appears when eyes are closed under the wakefulness condition but it disappears when eyes open and is replaced by beta rhythm [4], [5]. As shown in Fig. 1, three experts visually marked the start point s^1 and the end point e^1 of the ECE^1 in VEOG signal, which are equal to the start point and end point of continuous alpha waves in alpha blocking phenomenon in O2 signal. ECE^2 is defined as the eye closure event with alpha wave's attenuation-disappearance phenomenon, emerging a lot in the later stage of the simulated driving. For the alpha attenuation-disappearance phenomenon [3] (Fig. 1), the marked split point p^2 divided the ECE^2 into two phases: alpha attenuation phase and alpha disappearance phase. The start point s^2, split point p^2 and end point e^2 of ECE^2 were also visually marked. The start point s^2 and the end point p^2 of ECE^2 were equal to the start point and end point of alpha waves in the alpha attenuation phase of the alpha wave attenuation-disappearance phenomenon in O2 signal, respectively.

B. The Proposed Algorithm

For each subject's data, the first about 60-min consecutive data epoch, which contained at least 35 eye closure evens in the early stage of the driving, was used for training. The rest of the data was used for testing. In the training phase, the wavelet energy threshold and well-trained SVM model for each subject were obtained as follows:

Step 1: Obtaining wavelet energy threshold.

1) OPEN and CLOSE periods: In the training data, the numbers of the ECE^1 and ECE^2 were n_1 and n_2. The data periods without and with alpha waves in the whole training data period (marked as S) were respectively defined as the OPEN period and the CLOSE period: OPEN = $S - \left(\sum_{i=1}^{n_1} \cup [s_i^1, e_i^1]\right) \cup \left(\sum_{i=1}^{n_2} \cup [s_i^2, e_i^2]\right)$ and CLOSE = $\left(\sum_{i=1}^{n_1} \cup [s_i^1, e_i^1]\right) \cup \left(\sum_{i=1}^{n_2} \cup [s_i^2, p_i^2]\right)$.

2) Continuous wavelet transform (CWT): The complex Morelet wavelet [7] as a complex exponential modulated Gaussian function was selected to make CWT for the O2 signal due to its similar geometric shape to the alpha waves. Wavelet energy $w(t)$ in the fixed alpha frequency band F = [8, 12] Hz was calculated according to the wavelet coefficients $W(f_s, t)$:

$$w(t) = \int_F |W(f_s, t)|^2 df_s \tag{1}$$

where, f_s is the frequency parameter. After that, wavelet energy $w(t)$ was averaged in time window T. T is set to 1 s due to obvious short burst of alpha waves within 1 s.

$$E_w = \int_{t-T/2}^{t+T/2} w(t)dt \quad (2)$$

3) Wavelet energy threshold: The CWT using the complex Morlet mother wavelet at scales 1 to 1024 was applied to the O2 signal during the CLOSE or OPEN periods. According to Eq. (2), we obtained numerous 1-s alpha wavelet energy value samples for the CLOSE and OPEN periods, respectively. We calculated alpha wavelet energy threshold value E_{th} as the mean of the minimum level of alpha wavelet energy value distribution during the CLOSE period and the maximum level of that during the OPEN period.

Step 2: Training SVM model. The key to distinguish the two types of alpha-related phenomena was to distinguish the split point p^2 in ECE^2 from the end point e^1 in ECE^1. We marked a certain middle point of the ECE^1 in VEOG signal as a pseudo split point p^1 to compensate the lack of the real split point p^2, due to the similar VEOG signal waveforms around them.

1) Feature extraction: We respectively extracted Haar wavelet energy feature for each pair of points in two types of eye closure events: the pseudo and end points (p^1 and e^1) in ECE^1 and the split and end points (p^2 and e^2) in ECE^2. The Haar mother wavelet [8] has similar shape to the waveforms in VEOG signal and characterizing well abrupt transition caused by the behaviors of closing and opening eyes with relatively large wavelet coefficients around the upward and downward trend lines at all scales as illustrated in Fig. 1. By applying the CWT with the Haar wavelet at scales 1 to 128 to the 1-s VEOG signal before any (pseudo) split points (p^1) p^2 and end points (e^1 and e^2), we calculated the corresponding wavelet energy value for each scale to form a 128-dimensional Haar wavelet energy feature vector for each corresponding point.

2) Training linear SVM model: All the Haar wavelet energy feature vector samples corresponding to the (pseudo) split point (p^1) p^2 were labeled as the class "+1" and all those corresponding to the end points e^1 and e^2 were labeled as the class "-1". To classify the two classes, linear SVM [9] was used and the optimal parameter C was searched in the range [1, 1000] to find the best classification accuracy.

In the testing phase, we utilized the obtained alpha wavelet energy threshold E_{th} and the well-trained SVM model to realize tracking the change in alpha waves and detecting two types of alpha-related phenomena. The detail process and results for testing phase were given in the next session.

IV. Results

It is well known that the attenuation of alpha waves is the reliable indicator for sleep onset and alpha blocking phenomenon appears during relax wakefulness. Though different from the intermittent form of the attenuation of alpha wave in sleep process, the alpha wave attenuation-disappearance phenomenon also indicates the current undergoing sleep onset period in the eye closure events. These two alpha-related phenomena are supposed to represent two significant different sleepiness levels: sleep onset and relaxed wakefulness. In addition, we used box plot to analyzed the duration distribution of two types of ECEs corresponding to two alpha-related phenomena from eight subjects. The duration distribution of ECE^2 with the median value 9.9 s was higher than that of ECE^1 with the median value 2.8 s, indicating higher sleepiness level for the alpha wave attenuation-disappearance phenomenon.

After obtaining the individual wavelet energy threshold E_{th} and the well-trained SVM model, the testing phase was done for each corresponding subject and the numbers of two types of ECEs in each subject were shown in Table I. Fig. 1 illustrates the process for tracking the change in alpha waves and detecting the two types of alpha-related phenomena. At first, to realize real-time detection, we applied a 1-s time window length to the O2 signal. With forward sliding step length of 0.1 s, we applied the CWT to the 1-s window data in O2 signal to obtain the corresponding 1-s alpha wavelet energy value E_w (Eq. (2)). The current time point was defined as the middle time point of the current 1-s window data, due to the way for calculating alpha wavelet energy value in Eq. (2). The change in the alpha wavelet energy value E_w over time is shown in Fig. 1.

As soon as the current alpha wavelet energy E_w exceeded the threshold value E_{th} the current time point was determined as the start point s' of alpha waves (Fig. 1). After that, with forward sliding every 0.1 s, if the current wavelet energy value E_w was consistently higher than the threshold value E_{th}, the current time point indicated the consistent presence of alpha waves. Until the current E_w was lower than the threshold value E_{th}, the current point was judged as the end point of alpha waves. Once the current time point is judged as the end point of alpha waves, we further apply CWT with the Haar mother wavelet to the 1-s VEOG signal before the current time point (Fig. 1) to obtain the corresponding Haar wavelet energy feature vector. Then, the obtained SVM model from the training phase was used to further classify this feature vector as class "+1" or class "-1", equal to judging the current time point as a split point p' of ECE^2 (equal to the end point of alpha waves in alpha wave attenuation-disappearance phenomenon) or an end point e' of ECE^1 (equal to the end point of alpha waves in alpha blocking phenomenon).

If the start point s' or the end point e' (Fig. 1), which is determined by the detection algorithm, fall into the range [s^1(s^2)-0.5 s, s^1(s^2)+0.5 s] or [e^1-0.5 s, e^1+0.5 s] centered by a certain visually marked start point $s^1(s^2)$ or end point e^1, this point is considered to be correctly detected. If the split point p' determined by the detection algorithm fall into the range [p^2-0.8 s, p^2+0.8 s] centered by a certain visually marked split point p^2, this split point is considered to be correctly detected. The longer time range of 0.8 s was set due to the greater subjective bias for marking the split point. In order to investigate performance of the algorithm, we calculated the sensitivity (=TP/(TP+FN)) and precision (=TP/(TP+FP)) for the start point s^1 and end point e^1 in ECE^1 and the start point s^2 and split point p^2 in ECE^2. False positive (FP), true positive (TP) and false negative (FN) detection numbers were determined as the number of points (start points or end points

TABLE I

THE RESULTS FOR DETECTING THE DIFFERENT TYPES OF POINTS AND THE OVERLAPPING RATES BETWEEN THE DETERMINED PERIOD AND THE VISUALLY MARKED PERIOD

Subjects	#ECE^1	Start points (ECE^1)					End points (ECE^1)					Overlapping rate
		TP	FP	FN	Sensitive, %	Precision, %	TP	FP	FN	Sensitive, %	Precision, %	(ECE^1),%
1	20	20	1	0	100	95.2	20	1	0	100	95.2	99.8
2	18	17	1	1	94.4	94.4	17	1	1	94.4	94.4	97.1
3	26	25	2	1	96.2	92.6	25	2	1	96.2	92.6	97.5
4	15	15	1	0	100	93.8	15	1	0	100	93.8	99.5
5	29	28	4	1	96.6	87.5	28	2	2	93.3	93.3	96.4
6	31	29	1	2	93.6	96.7	27	1	4	87.1	96.4	93.3
7	14	11	1	3	78.6	91.7	12	1	2	85.7	92.3	90.1
8	22	20	2	2	90.9	90.9	21	2	1	95.4	91.3	93.5
Mean $\pm$ SD					93.8 $\pm$ 6.9	92.9 $\pm$ 2.9				94.0 $\pm$ 5.3	93.7 $\pm$ 1.7	95.9 $\pm$ 3.4
Subjects	#ECE^2	Start points (ECE^2)					Split points (ECE^2)					Overlapping rate
		TP	FP	FN	Sensitive, %	Precision, %	TP	FP	FN	Sensitive, %	Precision, %	(ECE^2), %
1	23	23	0	0	100	100	22	0	1	95.7	100	98.8
2	38	38	2	0	100	95	36	2	2	94.7	94.7	96.9
3	21	19	1	2	90.5	95	19	1	2	90.4	95	95.7
4	24	23	2	1	95.8	92	23	2	1	95.8	92	98.7
5	32	31	2	1	96.9	93.9	30	2	2	93.8	93.8	96.2
6	35	33	3	2	94.3	91.7	32	3	3	91.4	91.4	94.4
7	16	15	1	2	88.2	93.8	11	1	4	73.3	91.7	92.8
8	11	11	3	0	100	78.6	11	3	0	100	78.6	99.3
Mean $\pm$ SD					95.7 $\pm$ 4.5	92.5 $\pm$ 6.2				91.9 $\pm$ 8.0	92.2 $\pm$ 6.1	96.6 $\pm$ 2.3

or split points) wrongly detected, points correctly detected and missed points (genuine points not detected by the algorithm). From Table I we can see that the sensitivity and precision for the detections of the start and end points of ECE^1 are high across eight subjects with the mean values of 93.8% and 92.9% and the mean values of 94.0% and 93.7%, respectively. The sensitivity and precision for the detections of the start and split points of ECE^2 are also generally high across eight subjects, respectively with the mean values of 95.7% and 92.5% and the mean values of 91.9% and 92.2%.

Moreover, the period containing all the eye closure events which were determined as belonging to ECE^1 (Fig. 1) was expressed as: $P_{ECE_d^1} = [s_1', e_1'] \cup [s_2', e_2'] \cdots \cup [s_{n_1'}', e_{n_1'}']$. The corresponding visually marked period containing all the eye closure events of ECE^1 was expressed as: $P_{ECE_v^1} = ([s_1^1, e_1^1] \cup [s_2^1, e_2^1] \cdots \cup [s_{n_1}^1, e_{n_1}^1]$. The overlapping part between the determined period $P_{ECE_d^1}$ and the visually marked period $P_{ECE_v^1}$ indicated the consistent appearance of continuous alpha waves with eyes closed and the overlapping rate was calculated as $(P_{ECE_d^1} \cap P_{ECE_v^1})/P_{ECE_v^1}$. Similarly, the period containing all the epoches which were with alpha wave's attenuation and determined as belonging to the ECE^2 (Fig. 1) were described as: $P_{ECE_d^2} = [s_1', p_1'] \cup [s_2', p_2'] \cdots \cup [s_{n_2'}', p_{n_2'}']$, and the corresponding visually marked period consists of alpha attenuation phases in the ECE^2 was expressed as $P_{ECE_v^2} = [s_1^2, p_1^2] \cup [s_2^2, p_2^2] \cdots \cup [s_{n_2}^2, p_{n_2}^2]$. The overlapping part between the determined period $P_{ECE_d^2}$ and the visually marked period $P_{ECE_v^2}$ indicated the consistent appearance of the alpha waves with a little amplitude attenuation during eye-closed period and the corresponding overlapping rate was calculated as $(P_{ECE_d^1} \cap P_{ECE_v^1})/P_{ECE_v^1}$. As shown in Table I, the overlapping rates for the two types of eye closure events are generally high for all subjects, respectively with the mean values of 95.9 % and 96.6%.

V. CONCLUSIONS

The experimental results have shown that the proposed algorithm is feasible to detect the appearance of alpha waves during eye-closed period within 1 s and further determine the current sleepiness as the relaxed wakefulness or the sleep onset at the moment of the disappearance of alpha waves. Our algorithm with the use of a few electrode channels has important practical significance in designing a real-time wireless EEG-based device for driver sleepiness detection.

REFERENCES

[1] R. D. Ogilvie, "The process of falling asleep," Sleep Medicine Reviews, 2001, 5(3): 247-270, .

[2] M. H. Silber, S. Ancoli-Israel, M. H. Bonnet, S. Chokroverty, M. M. Grigg-Dammberger, M. Hirshkowitz, C. Iber, "The visual scoring of sleep in adults," J Clin Sleep Med, 2007, 3(2): 121-131.

[3] Y. Jiao, B.-L. Lu, "An Alpha Wave Pattern from Attenuation to Disappearance for Predicting the Entry into Sleep during Simulated Driving," The 8th International IEEE EMBS conference on Neural Engineering, 2017.

[4] J. L. Cantero, M. Atienza, and R. M. Salas, "Human alpha oscillations in wakefulness, drowsiness period, and REM sleep: different electroencephalographic phenomena within the alpha band," Clinical neurophysiology, 2002, 32.1:54.

[5] C. J. Harland, T. D. Clark, R. J. Prance, "Remote detection of human electroencephalograms using ultrahigh input impedance electric potential sensors," Applied Physics Letters, 2002, 81(17), 3284-3286.

[6] M. W. Johns, "A new method for measuring daytime sleepiness: the Epworth sleepiness scale," Sleep, 1991, 14(6): 540-545.

[7] A. N. Pavlov, A. E. Hramov, A. A. Koronovskii, E. Y. Sitnikova, V. A. Makarov, and A. A. Ovchinnikov, "Wavelet analysis in neurodynamics," *Physics-Uspekhi*, 2012, 55(9), 845.

[8] C. F. Chen, C. H. Hsiao, "Haar wavelet method for solving lumped and distributed-parameter systems," IEE Proceedings-Control Theory and Applications, 1997, 144(1), 87-94.

[9] T. Joachims, "Text categorization with support vector machines: Learning with many relevant features,", Machine learning: ECML-98, 1998, 137-142.